Parasitol Res (2005) 97: 13–20
DOI 10.1007/s00436-005-1359-x

ORIGINAL PAPER

T. Boonmars · Z. Wu · I. Nagano · Y. Takahashi

Trichinella pseudospiralis infection is characterized by more continuous and diffuse myopathy than *T. spiralis* infection

Received: 18 January 2005 / Accepted: 23 March 2005 / Published online: 10 June 2005

Abstract A time course study was performed to reveal the sequence of histopathology after *Trichinella spiralis* or *T. pseudospiralis* infection in mice. A cyst was formed in the former case by about 18 days post infection and prominent myopathy was restricted within the cyst. In the latter case, however, no typical cyst was formed, and myopathy spread diffusely over the infected muscle tissues occupying half the area of muscle sections. An electron microscope observation revealed that the disintegration of muscle cells was delayed in *T. pseudospiralis* infection than in *T. spiralis* infection. Quantitative reverse transcription polymerase chain reaction (RT-PCR) showed that apoptosis-related genes were expressed for a longer term in muscles infected with *T. pseudospiralis* than in those with *T. spiralis*, although the same spectrum of genes are mobilized. Examined apoptosis-related genes included tumor suppressor genes p53, p53; mouse double minute 2, MDM2; cyclin-dependent kinase inhibitor p21 (WAF1), $p21^{waf}$; Bcl-2 associated protein X, BAX; apoptotic protease activating factor 1, Apaf-1; Caspase 9 and serine/ threonine protein kinase, PKB. Micro-dissection of the infected muscle tissue and subsequent RT-PCR confirmed that the expressions of these genes are restricted to tissue with myopathy. Thus, the expression of the apoptosis-related genes correlated with continuous and diffuse myopathy caused by *T. pseudospiralis* infection.

Introduction

Following oral infection, the larvae of *Trichinella spiralis* at the muscle stage grow to adult hood and deliver the next generation (newborn larvae) which invade the skeletal muscle and establish parasitism, forming their residence (the capsule). The inflammatory reaction occurs around the capsule, resulting in local muscular change (myopathy), which is a major clinical symptom of trichinellosis. The capsule formation is completed by about 18 days after the infection, and subsequently myopathy tends to reduce gradually although the parasite continues its parasitism for years.

T. pseudospiralis is another major species of the genus *Trichinella*. The life cycle is essentially the same as that of *T. spiralis*, but this species has also received a great deal of attention because the two species differ in their biologically intriguing points. Unlike *T. spiralis* infected muscle cells, the *T. pseudospiralis* infected muscle cell does not form septum to seal off the damaged area, as such the whole length of the infected muscle cell is affected (Wu et al. 2001).

Another difference is satellite cell response. Satellite cells (myoblasts) proliferate in response to muscle cell damage caused by *Trichinella* infection as in the case of repairing other kinds of muscle damage (Wu et al. 2001). In normal repair processes, the proliferated satellite cells differentiate to new muscle cells and fuse with the damaged muscle cells (Bischoff 1994), but in the case of *Trichinella* infection, they misdifferentiate to a different cell, named the nurse cell (Wu et al. 2001). The new nurse cell fuses with the infected muscle cell in the case of *T. spiralis* infection.

Thus, the comparison of the two species seems to provide an excellent experimental model to dissect molecular mechanisms that govern muscle cell transformation as well as myositis associated with trichinellosis.

In previous reports, we showed the temporal elevation of apoptosis-related-gene expression with association to the capsule formation in *T. spiralis* infected muscles, during which time myositis begins to be obvious. Pro-apoptosis genes (BAX, Caspase9 and Apaf-1) are expressed in the basophilic cytoplasm (infected muscle cell origin), which soon dies through the apoptosis, and anti-apoptosis factor (PKB) is in the eosinophilic cytoplasm

T. Boonmars · Z. Wu · I. Nagano · Y. Takahashi (✉)
Department of Parasitology, Gifu University School of Medicine, Yanagido1-1, Gifu 501-1194, Japan
E-mail: yu3@cc.gifu-u.ac.jp
Tel.: +81-58-2306366
Fax: +81-58-2306368

(satellite cell origin), which can survive for a longer time. The elevation of apoptosis-related factors and severity of myositis are associated although there are no direct cause–result relations.

In this study, for further understanding of myopathy caused by *T. pseudospiralis* infection, the kinetics of expression of apoptosis-related genes was investigated with comparison of histopathological findings. A panel of the analyzed genes was expanded more than in the previous study, which included tumor suppressor genes p53, p53; mouse double minute 2, MDM2; cyclin-dependent kinase inhibitor p21 (WAF1), $p21^{waf}$; Bcl-2 associated protein X, BAX; apoptotic protease activating factor 1, Apaf-1, Caspase 9, and serine/threonine protein kinase, PKB.

Materials and methods

Parasites and infection

Trichinella spiralis (ISS413) and *T. pseudospiralis* (ISS13) have been maintained in mice at our laboratory. Nude mice purchased from Chubu Kagaku Shizai Co., Ltd (Japan) were orally infected with *T. spiralis* or *T. pseudospiralis* (800 infective larvae per mouse). The mice were killed at certain time points (0, 8, 13, 18, 28, 33, 38, 43, and 90 days post infection (dpi)).

Light microscopic and electron microscopic observation

Striated muscle tissues infected with *T. pseudospiralis* or *T. spiralis* were processed for light microscopic and electron microscopic observation at 0, 8, 13, 18, 28, 33, 38, 43, and 90 dpi according to the well established manner (Takahashi et al. 1988). In brief, for light microscopic observation, striated muscle tissue was fixed in 10% formalin, embedded in paraffin, thin-sectioned, and stained with hematoxylin and eosin (H&E staining). The muscle tissue was processed for electron microscopic observation with fixation of 2.5% glutaraldehyde plus 4% paraformaldehyde, and double staining with uranyl acetate and Raynold's solution.

Primer design for quantitative RT-PCR

The primer pairs for pro-apoptosis factors (p53, MDM2, $p21^{waf}$, BAX, Apaf-1, and Caspase 9) and anti-apoptosis factors (PKB) were designed based on the published sequence as summarized in Table 1.

The primer pairs for endogenous controls (mouse glyceraldehyde-3-phosphate dehydrogenase, MG3PDH, and 18S rRNA) were designed based on the published sequence as summarized in Table 2.

RNA isolation from infected muscles and RT-PCR to detect apoptosis-related genes

Anesthetized mice were killed by means of cervical dislocation and quickly dissected. Whole muscle tissues (150 mg) obtained from the hind limbs of 8, 13, 18, 23, 28, 33, 38, and 43 dpi of *T. pseudospiralis* infection were used for analysis. Uninfected mouse muscles were used as a control. Total RNA was isolated using TRIZOL (Invitrogen, USA) according to the manufacturer's instructions. The isolated RNA was treated with DNase (5 units of RQ1 RNase-Free DNase, Promega, USA) and 119 units of Ribonuclease Inhibitor (Takara Shuzo, Japan) in the buffer (400 mM Tris–HCl, 100 mM NaCl, 60 mM $MgCl_2$, and 20 mM ditheothreitol, pH 7.5). The total RNA was extracted with phenol/chloroform, precipitated with ethanol, and dissolved in RNase-free water (100 µl). The resulting RNA was reverse transcribed into cDNA using Oligo(dT)12–18 primers (Amersham Phamacia Biotech, USA) and a Ready-to-Go First-Strands beads kit (Amersham Phamacia Biotech). Thirty-two microlitres of the RNA sample (4.3 µl of RNA original) and 1 µl of 0.5 µg/µl Oligo(dT)12–18

Table 1 Summary of the primer pairs for apoptosis-related genes (p53, MDM2, $p21^{waf}$, BAX, Apaf-1, Caspase 9, and PKB)

Gene	Product Length (bp)	Sequence upper line: forward primer bottom line: reverse primer	GenBank accession number/ reference
PKB	551	5′-GGCAGGAAGAAGAGACGATG-3′ 5′-ACAGCCCGAAGTCCGTTAT 3	Boonmars et al. (2004b)
BAX	419	5′-CACCTGAGCTGACCTTGGAG-3′ 5′-GAGGACTCCAGCCACAAAGA-3′	Boonmars et al. (2004b)
Apaf-1	575	5′-ATCCTGGTGCTTTGCCTCTA-3′ 5′-TACACCCCCTGAAAAGCAAC-3′	Boonmars et al. (2004b)
Caspase 9	474	5′-ACCAATGGGACTCACAGCAA-3′ 5′-AGGATGACCACCACAAAGCA-3′	Boonmars et al. (2004b)
p53	303	5′ACAGGACCCTGTCACCGAGACC 3 5′-GACCTCCGTCATGTGCTGTGAC-3′	Vaslet et al. (2002)
MDM2	422	5′AGGTCTATCGGGTCACAGTC-3′ 5′-CTCTTTCACGCTTTCTTGG-3′	U47934
$p21^{waf}$	356	5′CGAGAACGGTGGAACTTTGA-3′ 5′TGGGCACTTCAGGGTTTTC-3′	U24173

Table 2 Summary of the primer pairs for endogenous controls (mouse glyceraldehydes-3-phosphate dehydrogenase, MG3PDH, and 18S rRNA)

Gene	Product length (bp)	Sequence upper line: forward primer bottom line: reverse primer	GenBank accession number
MG3PDH	728	5′-CCCGTAGACAAAATGGTGAAGG-3′ 5′-GACACATTGGGGGTAGGAACAC-3′	Boonmars et al. (2004b)
18S rRNA	549	5′-AGATCAAAACCAACCCGGTGAG-3′ 5′-GGTAAGAGCATCGAGGGGGC-3′	Boonmars et al. (2004b)

primers were added to a Ready-to-Go tube. The tube was incubated at 37°C for 60 min and then 95°C for 10 min.

The PCR reaction mixture comprised 3 μl of reverse transcription products (1:10 diluted), 3 μl of 10x PCR buffer, 3 μl of deoxynucleoside triphosphate (2.5 mM each), 6 μl of primer pairs (5 μM), 0.12 μl of *Taq* polymerase (5 U/μl, Takara Shuzo), and 15 μl of distilled water to give the final volume of 30 μl. PCR conditions are summarized in Table 3.

Aliquots of PCR products were run for gel electrophoresis and photographed under UV light. The photographs were analyzed for density using the Scion image software (Scion, USA). All reactions for the standard control and the experiment sample were performed in triplicate. The amounts of p53, MDM2, $p21^{waf}$, BAX, Apaf-1, Caspase 9, and PKB genes were calculated as follows:

$$\text{The amount of sample gene} = \frac{\text{gene sample / MG3PDH of sample}}{\text{gene control / MG3PDH of control.}}$$

The ratio of density of the apoptosis-related genes and the standard gene were plotted in a graph (Fig. 3).

Laser capture microscopy to isolate RNA from the capsule and RT-PCR

Cryosections (8 μm in thickness) of quickly frozen muscles at 18 dpi were prepared and placed onto glass slides (preheated at 200°C for 2 h to destroy RNase) and dried immediately with room air using a conventional dryer. The infected muscle cells were micro-dissected out using the laser micro-beam of the Robot-MicroBeam system (P.A.L.M., Germany) equipped with a 40x dry long-distance objective lens. The control cells were collected from the unaffected area of the same sample used for the experiment. The infected muscle cells were cut together with their supporting optimal cutting temperature compound with a laser beam. One microliter of mineral oil was dropped into a 0.5 ml tube cap. The test samples contained about 1×10^6 μm^2 of tissue section, and the control was prepared from the unaffected muscle with the same square μm.

Total RNA was isolated using an RNeasy protect mini kit (Qiagen GmbH, Germany). The caps of 0.5 ml tubes were reversed, and the lysis buffer was added. After the incubation in a water bath for 15 min at 37°C with a vigorous vortex for 30 min following the manufacturer's protocol, 32 μl of the RNA sample was reverse transcribed into cDNA using 1 μl of 0.5 μg/μl oligo(dT)12–18 primers (Amersham Phamacia Biotech) and a Ready-to-Go First-Strands beads kit (Amersham Phamacia Biotech). The tube was incubated at 37°C for 60 min and then 95°C for 10 min. To prevent mRNA degradation, every step was performed on ice, and all equipment and water were treated with DEPC.

The PCR reaction mixture comprised 3 μl of the reverse transcription products, 1.5 μl of 10x PCR buffer, 1.5 μl of deoxynucleoside triphosphate (2.5 mM each), 3 μl of primer pairs (5 μM), 0.06 μl of *Taq* polymerase (5 U/μl), and 6 μl of distilled water to give a final volume of 15 μl. PCR conditions are summarized in Table 4.

Table 3 Summary of the RT-PCR condition for apoptosis-related gene in infected muscle

Gene	PCR condition	Cycle
MG3PDH	94°C for 30 s, 56°C for 30 s, 72°C for 2 min	22
BAX	94°C for 30 s, 56°C for 30 s, 72°C for 2 min	38
Apaf-1, Caspase 9	94°C for 30 s, 56°C for 30 s, 72°C for 2 min	40
PKB	94°C for 30 s, 56°C for 30 s, 72°C for 2 min	28
p53	94°C for 30 s, 59°C for 30 s, 72°C for 2 min	28
MDM2, $p21^{waf}$	94°C for 30 s, 59°C for 30 s, 72°C for 2 min	40

Table 4 Summary of the RT-PCR condition for apoptosis-related gene in capsule or unaffected muscle cell

Gene	PCR condition	Cycle
MG3PDH, BAX, Apaf-1, Caspase 9, PKB	94°C for 30 s, 56°C for 30 s, 72°C for 2 min	35
p53, MDM2, $p21^{waf}$	94°C for 30 s, 59°C for 30 s, 72°C for 2 min	35

The amount of each gene was calculated according to the method described above.

Immunohistochemistry

To identify the expression site of some of the apoptosis factors (Caspase 9, Apaf-1 and PKB), an in situ localization study was performed employing immunoperoxidase staining on cryosections of the infected muscle tissues (23 and 48 dpi). The first antibodies were purchased from Santa Cruz Biotechnology Inc.(Santa Cruz, USA). Staining details were reported in our previous paper (Boonmars et al. 2004b).

Results

Histology of *Trichinella* infection

The result with *T. spiralis* infection was nearly the same as those previously published (Matsuo et al. 2000; Wu et al. 2001). Therefore, only a brief summary is described here with emphasis on the damaged muscle areas. After entrance by NBL of *T. spiralis*, the muscle cell transformed into the nurse cell, which is indicated by the basophilic profile in H&E staining (Fig. 1a, b). Severe damaged areas surrounding the larva were observed at 13 dpi (Fig. 1a) and at 18 dpi (Fig. 1b). At 28 (Fig. 1c),

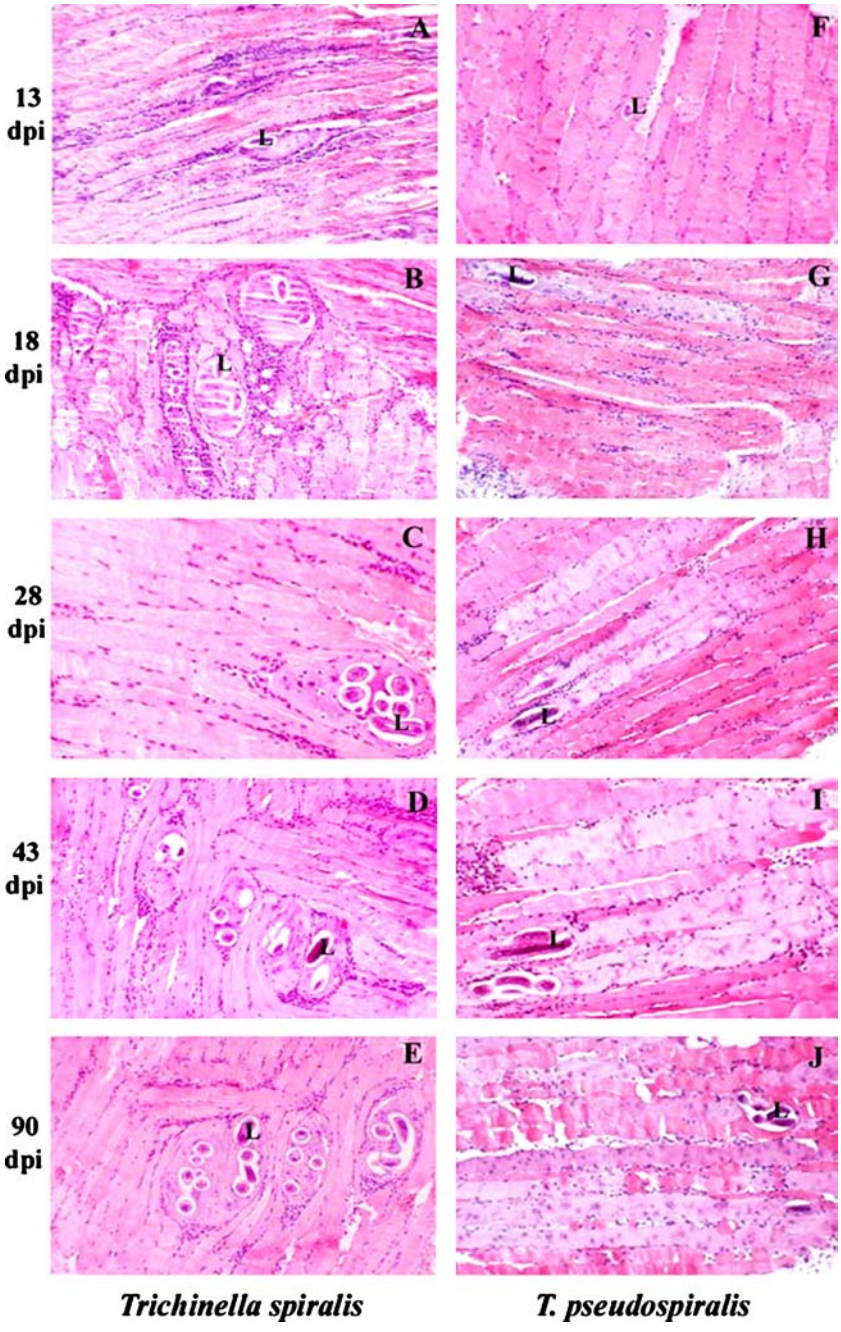

Fig. 1 Hematoxylin and eosin staining of *Trichinella spiralis* infected muscles (13 (**a**), 18 (**b**), 28 (**c**), 43 (**d**) and 90 (**e**) days post infection, dpi) and *T. pseudospiralis* infected muscles (13 (**f**), 18 (**g**), 28 (**h**) , 43 (**i**) and 90 (**j**) dpi). *L* larva. Original magnification, 100×

43 dpi (Fig. 1d), and 90 dpi (Fig. 1e), the damaged areas were restricted around the capsule.

After entrances by NBL of *T. pseudospiralis*, the infected muscle cells transformed in to the nurse cell but never had basophilic cytoplasm (Fig. 1f, g, h, i, j). On 13 dpi (Fig. 1f) and 18 dpi (Fig. 1g), a few damaged areas were observed in the muscle cells surrounding the larva. On 28 dpi (Fig.1h), the damaged area began to spread along the axis of infected muscle cells. Along with the infection time, the damaged areas were more increased in size, which is depicted in 43 dpi (Fig. 1i). The capsule wall and septum formation were undetectable under a light microscope. The basophilic cytoplasm remained undetectable (Fig. 1j) until the end of observation (90 dpi) in this study. The infected cell and or the damaged muscle areas were spread along its entire length as shown in Fig. 1j.

The ultrastructure of mature nurse cells of *T. pseudospiralis* has already been studied by our research group, reporting that the subcellular architecture of mature nurse cells is very similar (Xu et al. 1997). Therefore, this paper deals only with ultrastructural pathology at an early phase of the infection.

Figure 2 shows the ultrastructure of *T. pseudospiralis* infected muscle cells at 23 dpi. At this time point, the larva (upper right of the picture) has achieved its growth in the muscle cell and is supposedly already infective.

The infected muscle cells lost their typical subcellular integrity. There were numerous remnants of actin–myosine structure scattered in the cytoplasm of infected muscle cells. Rough endoplasmic reticulum was not prominent.

The area shown in Fig. 2 is adjacent to the parasite and supposedly the most severely damaged area. But the ultrastructural pathology resembles only that seen at 8 dpi of *T. spiralis* infection, which indicates that the pathological change in *T. pseudospiralis* is delayed in timing.

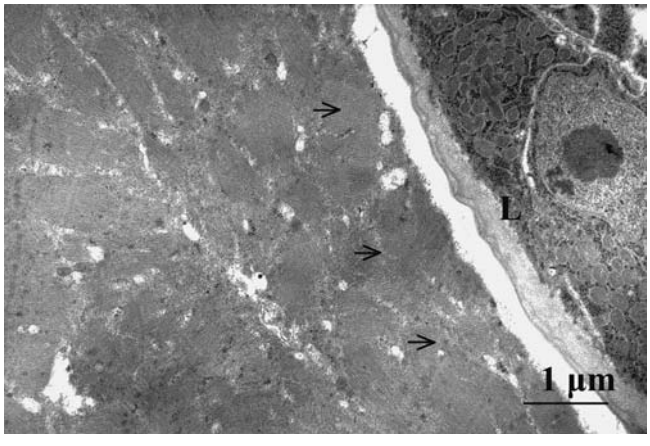

Fig. 2 Electron micrograph showing histopathology of a *Trichinella pseudospiralis* (right side) infected muscle on 23 dpi. *L* larva. The myofibrils are losing their integrity (arrow). *Bar* = 1 μm

Kinetics of expression of apoptosis-related-genes

Figure 3 shows the level of gene expression of apoptosis-related-genes determined by RT-PCR at various stages in infected muscles or non-infected muscles (RNA was isolated from block specimens). The specific band of MG3PDH (endogenous control) was observed at all stages with the band being the same density. Specific bands of p53, $p21^{waf}$, MDM2, BAX, Apaf-1, Caspase 9, and PKB were also observed in all stages of infection, but the expression level at each stage was different. The expression levels of p53, $p21^{waf}$, mdm2, BAX, and

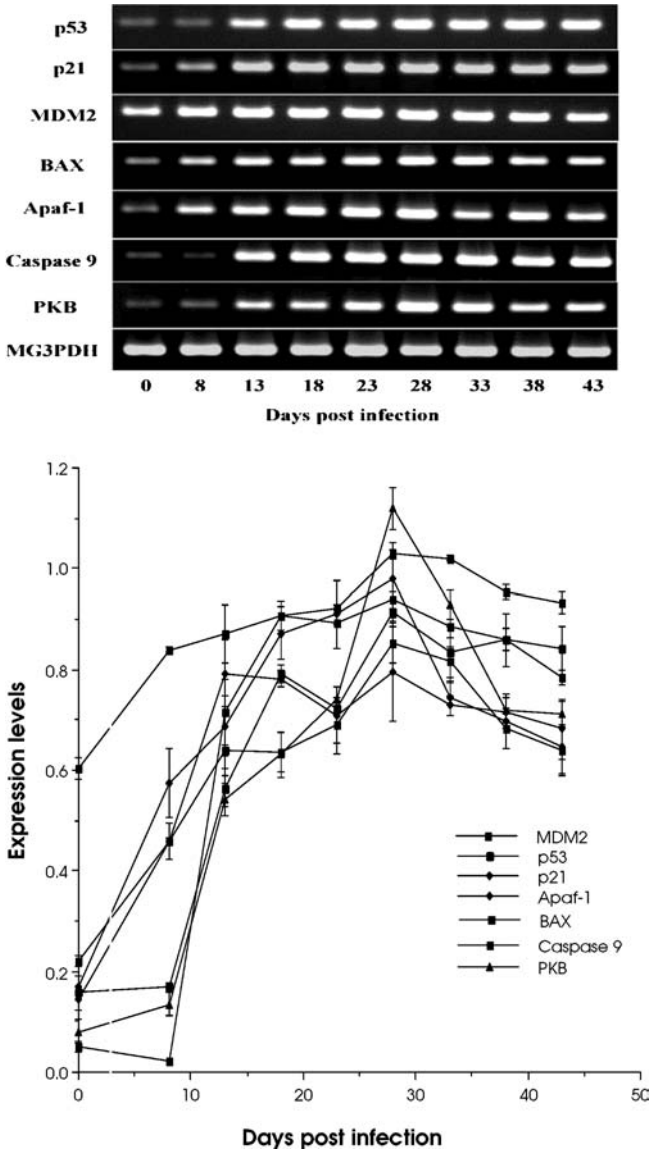

Fig. 3 RT-PCR results on expression level of apoptosis-related genes (p53, MDM2, $p21^{waf}$, BAX, Apaf-1, Caspase 9, and PKB) in the infected muscle tissue. Total RNA was isolated from infected muscle tissue at various stages (0, 8, 13, 18, 23, 28, 33, 38, and 43 days post infection) and amplification products were analyzed by agarose gel electrophoresis (*upper panel*). Using Scion Image software, the relative density of each sample band against the control band (MG3PDH) was analyzed (*lower panel*)

Apaf-1 were increased from 13 dpi and reached a peak at 28 dpi. After 28–43 dpi, those genes, expression levels showed some decrease but seemed to remain high. Expression levels of p53, Caspase 9, and PKB followed the same kinetics as $p21^{waf}$, MDM2, BAX, and Apaf-1, although the initial increase was somewhat delayed in timing.

DNA contamination in RNA samples was neglected by control PCR with the same primers, which resulted in the absence of the specific bands.

Detection of apoptosis-related-genes in the infected muscle cell

To determine whether the origin of p53, $p21^{waf}$, MDM2, BAX, Apaf-1, Caspase 9, and PKB genes is from nurse cells and/or muscle cells, RT-PCR was performed to detect the mRNA expression in nurse cells and muscle cells separately.

Figure 4 shows the RT-PCR results of the test genes (p53, $p21^{waf}$, MDM2, BAX, Apaf-1, Caspase 9, PKB) and the endogenous control gene (18S rRNA) at 18 dpi in the nurse cell sample and/or the muscle cell sample. A specific band of 18S rRNA (control) was observed in both samples with the same density. Specific bands of $p21^{waf}$, MDM2, BAX, and PKB were also observed in both samples, but the higher expression level of $p21^{waf}$, MDM2, BAX, and PKB was observed in the capsule sample, and a lower expression level was observed in the muscle cell sample. On the other hand, a specific band of p53 was observed only in the capsule sample. Apaf-1 and Caspase 9 product bands were not observed in either sample. Data in number and means are summarized in Table 5.

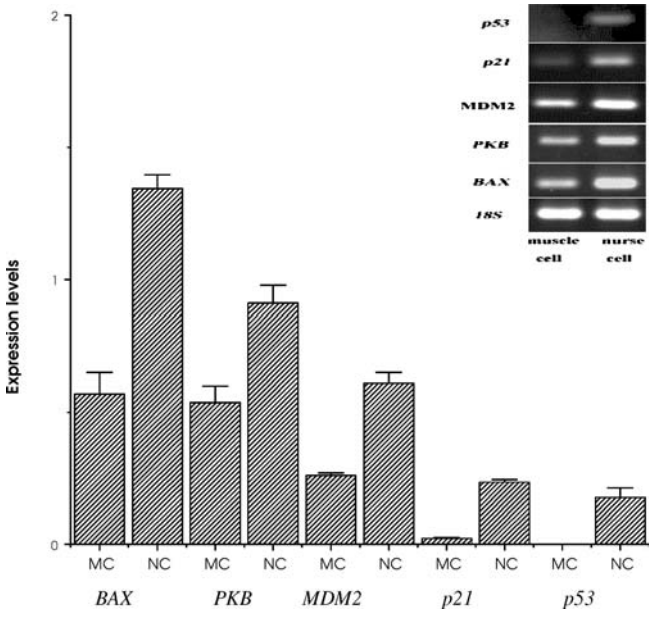

Fig. 4 RT-PCR results on expression level of apoptosis-related genes (p53, MDM2, $p21^{waf}$, BAX, and PKB) in the nurse cells or unaffected muscle cells which were obtained from *Trichinella pseudospiralis* infected mouse at 18 days post infection. Total RNA was isolated from laser microdissected infected muscle cells or unaffected muscle cells (control), amplification of the sample genes (p53, MDM2, $p21^{waf}$, BAX, and PKB) and the standard gene (18 S rRNA) was performed, and PCR products were analyzed by agarose gel electrophoresis (*right panel*). Using Scion Image software, the relative density of each sample band against the control band was analyzed and shown in the *left panel*. *MC* muscle cell, *NC* nurse cell

The in situ localization of apoptosis-related factors

Positive staining for the apoptosis-related factors (Caspase 9, Apaf-1, and PKB) was observed in the muscle cells infected with *T. pseudospiralis*, although there was some variability in the staining intensity within the same muscle cell. The immunostaining intensity was somewhat weaker in the 48-dpi sample than in the 23-dpi sample (Fig. 5).

Discussion

This study describes the chronology of histopathological change in *Trichinella* infected muscle tissues. Direct comparison of the histopathology between the two kinds of *Trichinella* species revealed intriguing differences between the two species that *T. pseudospiralis* causes diffuse and prolonged myopathy than *T. spiralis* does. In this paper, we refer to myopathy as muscle cell changes including disintegration of its striation and transformation to the nurse cell, which can be histopathologically defined. Myositis is defined by mononuclear cell infiltration.

In *T. spiralis* infection, the infected cell undergoes basophilic change, and is transformed to a nurse cell (Blotna-Filipiak et al. 1998; Wranicz et al. 1998). The cyst formation was completed at 18 dpi, and after cyst completion the myopathy was restricted within the cyst. Local myositis is seen around the cyst especially at the pole ends.

In *T. pseudospiralis* infection, the first morphological sign of myopathy, is the disturbance of striated structure. This myopathy begins from the vicinity of the parasite and spreads to periphery of the infected muscle cells, and finally the entire length of the cells is affected with myopathy. The septum is formed in *T. spiralis* infected muscle cells, which primarily functions to restrict spreading of myopathy (Wu et al. 2001). The lack of septum formation in *T. pseudospiralis* infection, however, seems to allow the myopathy to spread to the whole length of the cells.

After the *T. pseudospiralis* infection, muscle cells are affected and gradually transformed to the nurse cell. As shown in Fig. 1j at 90 dpi, more than 50% of the muscle cells are affected with myopathy; some areas have already been transformed to cytoplasm of a nurse cell. Thus, the histopathology of *T. pseudospiralis* infection is

Table 5 Summary of data in number and means of apoptosis-related gene expressed in capsule or unaffected muscle cell

Gene	BAX	PKB	MDM2	p21	p53
Muscle cell	0.566 ± 0.088	0.538 ± 0.059	0.261 ± 0.009	0.019 ± 0.005	0 ± 0
Nurse cell	1.342 ± 0.054	0.912 ± 0.066	0.6084 ± 0.042	0.235 ± 0.011	0.175 ± 0.041

Values are density ± SD

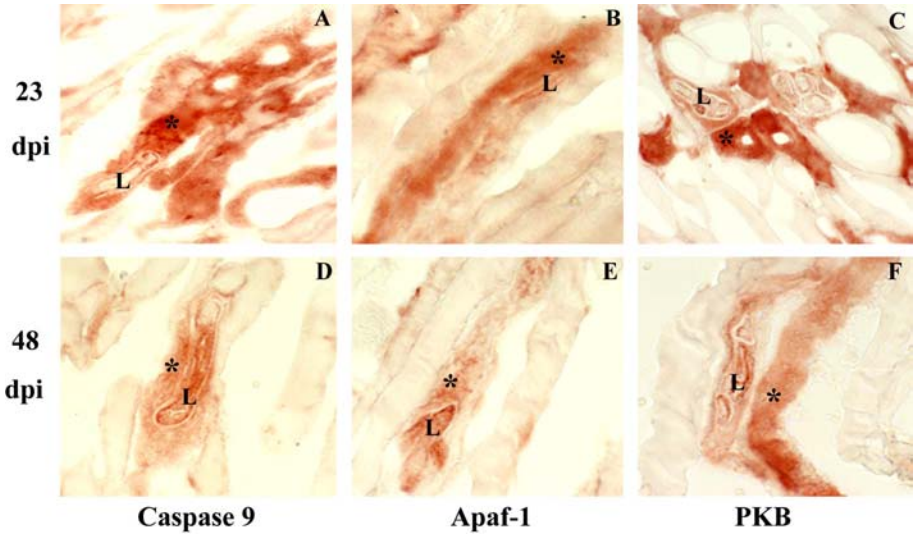

Fig. 5 The in situ localization of apoptosis-related factors in the muscle cells infected with *Trichinella pseudospiralis* at 23 and 48 days post infection. Caspase 9 (**a**, **d**), Apaf-1 (**b**, **e**), and PKB (**c**, **f**) were observed in infected muscle cell. *L* larva. *Asterisk* Red color is positive stained

characterized by diffuse myopathy. Along the cells with myopathy, mononuclear cells are infiltrated, suggesting the presence of myositis.

This diffuse myopathy is more prominent in *T. pseudospiralis* infection than in *T. spiralis* infection, but the reason is not the increased number of parasites infected in the former in comparison to the latter. More parasites are recovered from *T. spiralis* infected mice than *T. pseudospiralis* infected ones in the experiment where the same numbers of parasites are administered (our unpublished data). Two reasons for this can be postulated. Firstly, the whole length of the infected muscle cell is affected, consequently the myopathy becomes larger in area more than in the case with *T. spiralis* infection. Secondly, the activated satellite cells (myoblast) do not differentiate to the muscle cells, but to cells which are morphologically indistinguishable from the nurse cell with parasites.

Another characteristic of pathology in *T. pseudospiralis* infection is that myopathy occurs more slowly than in that of *T. spiralis* infection. A typical example is shown by Fig. 2 which is an electron micrograph of the *T. pseudospiralis* infected muscle cell obtained at 23 dpi. The cytoplasm is certainly affected but the sarcomere of the muscle cell still remains. This level of myopathy is equivalent to what is seen at the early phase of infection (10 dpi) with *T. spiralis* (Matsuo et al. 2000).

The nurse cell at its completion resembles that of *T. spiralis* (Xu et al. 1997), but the process towards nurse cell formation takes time, as in the case of *T. pseudospiralis* infection shown by histopathological investigations. This delay in completion seems to be in good concordance with our previous observation, which reported that the appearance of ACP is delayed and expression of ALP continues longer (Boonmars et al. 2004a). Thus, prolonged myopathy seems to be one of the characteristics of the *T. pseudospiralis* infection.

The expression of apoptosis-related genes remained high during the present experimental observation time, which is in contrast to the temporal increase seen in *T. spiralis* infection. The expression of apoptosis-related genes and myopathy are correlated although the mechanisms of correlation remain to be elucidated.

In *T. spiralis* infection, the basophilic cytoplasm expresses pro-apoptosis factors and dies quickly, but eosinophilic cytoplasm expresses both pro-apoptosis and anti-apoptosis factors and continues to survive for a longer time(Boonmars et al. 2004b). These apoptosis-related genes are expressed during the formation of the cyst, probably playing some role in the transformation of muscle cells.

The transformation of muscle cells leading to the nurse cell formation is a complex process involving a wide variety of apoptosis-related genes, and at least the entire panel of factors examined in this study is mobilized. In *T. pseudospiralis* infection, eosinophilic nurse cells express both pro-apoptosis and anti-apoptosis factors as shown by the present RT-PCR and immunoperoxidase staining results. Interaction between pro-apoptosis and anti-apoptosis factors may result in a

longer survival of the nurse cell. *T. pseudospiralis* enters the muscle cell and continues to parasitism in that cell. As such, it is advantageous for the parasites that the infected cell continues to survive. If the infected muscle cells die, the parasite cannot survive. In this sense, the longer survival of the nurse cell is very explainable.

As classically known, *T. spiralis* is an encapsulating species and *T. pseudospiralis* is not. The present study reported the additional difference that *T. pseudospiralis* infection is characterized by more prolonged and diffuse myopathy than *T. spiralis* infection. These differences in host responses are likely due to the differences of excretory-secretory products, especially stichosomal excretion granules which are introduced in the cytoplasm of infected muscle cells. Cloning and characterization of stichosomal protein are in progress at some laboratories, which resulted in the discovery of functional proteins including DNase (Mak and Ko 1999; Mak et al. 2000), serine protease (Nagano et al. 2003), and the proteinase inhibitor (Nagano et al. 2001). We have already cloned 43 and 53 kDa stichosomal proteins of both *T. spiralis* and *T. pseudospiralis*. A trial to correlate molecular differences in amino acid residues and phenotypic differences observed in this study are is in progress in our laboratory.

Acknowledgements This study was partially supported by a Grant-in-Aid for Scientific Research (15590366) from the Ministry of Education, Culture, Sports, Science and Technology of Japan.

References

Bischoff R (1994) The satellite cell and muscle regeneration. In: Engel AG, Armstrong CF (eds) Myology. McGraw-Hill INC Press, New York, pp 97–109

Blotna-Filipiak M, Gabryel P, Gustowska L, Kucharska E, Wranicz MJ (1998) *Trichinella spiralis*: induction of the basophilic transformation of muscle cells by synchronous newborn larvae. II. Electron microscopy study. Parasitol Res 84:823–827

Boonmars T, Wu Z, Nagano I, Nakada T, Takahashi Y (2004a) Differences and similarities of nurse cells in cysts of *Trichinella spiralis* and *T. pseudospiralis* . J Helminthol 78:7–16

Boonmars T, Wu Z, Nagano I, Takahashi Y (2004b) Expression of apoptosis-related factors in muscles infected with *Trichinella spiralis* . Parasitology 128: 323–332

Mak CH, Ko RC (1999) Characterization of endonuclease activity from excretory/secretory products of a parasitic nematode, *Trichinella spiralis*. Eur J Biochem 260:477–481

Mak CH, Chung YY, Ko RC (2000) Single-stranded endonuclease activity in the excretory–secretory products of *Trichinella spiralis* and *Trichinella pseudospiralis*. Parasitology 120:527–533

Matsuo A, Wu Z, Nagano I, Takahashi Y (2000) Five types of nuclei present in the cyst of *Trichinella spiralis*. Parasitology 121:203–210

Nagano I, Wu Z, Nakada T, Matsuo A, Takahashi Y (2001) Molecular cloning and characterization of a serine proteinase inhibitor from *Trichinella spiralis*. Parasitology 123:77–83

Nagano I, Wu Z, Nakada T, Boonmars T, Takahashi Y (2003) Molecular cloning and characterization of a serine proteinase gene of *Trichinella spiralis*. J Parasitol 89:92–98

Takahashi Y, Uno T, Furuki J, Yamada S, Araki T (1988) The morphology of *Trichinella spiralis*: ultrastructural study of mid- and hindgut of the muscle larvae. Parasitol Res 75: 19–27

Vaslet CA, Messier NJ, Kane AB(2002) Accelerated progression of asbestos-induced mesotheliomas in heterozygous p53 + /- mice. Toxicol Sci 68:331–338

Wranicz MJ, Gustowska L, Gabryel P, Kucharska E, Cabaj W (1998) *Trichinella spiralis:* induction of the basophilic transformation of muscle cells by synchronous newborn larvae. Parasitol Res 84:403–407

Wu Z, Matsuo A, Nakada T, Nagano I, Takahashi Y (2001) Different response of satellite cells in the kinetics of myogenic regulatory factors and ultrastructural pathology after *Trichinella spiralis* and *T. pseudospiralis* infection. Parasitology 123:85–94

Xu D, Nagano I, Takahashi Y (1997) Electron microscopic observations on the normal development of *Trichinella spiralis* from muscle larvae to adult worms in BALB/c mice with emphasis on the body wall, genital organs and gastrointestinal organs. Electron Microsc (Tokyo) 146:347–352